Journal of CO2 Utilization 53 (2021) 101712

Contents lists available at ScienceDirect

Journal of CO2 Utilization

journal homepage: www.elsevier.com/locate/jcou

Microfluidic analysis of seawater-based CO_2 capture in an amine solution with nickel nanoparticle catalysts

Abhishek Ratanpara [a,b], Alexander Shaw [a], Mallory Thomas [a], Rajesh N. Patel [b], Myeongsub Kim [a,*]

[a] Ocean and Mechanical Engineering, Florida Atlantic University, 777 Glades Road, Boca Raton, FL, 33431, United States
[b] Institue of Technology, Nirma University, Ahmedabad, Gujarat, 382481, India

ARTICLE INFO

Keywords:
CO_2 capture
Post-combustion carbon capture
Seawater
Monoethanolamine
Nickel nanoparticles

ABSTRACT

Post-combustion CO_2 capture methods like amine scrubbing are currently being utilized to reduce CO_2 emissions from fossil fuel power plants. Aqueous monoethanolamine (MEA) solutions are typically used in these processes due to their high CO_2 absorption capacity and rapid reaction rate, but these solutions also produce environmentally harmful toxic wastewater and consume large amounts of freshwater. This research analyzes the effectiveness of seawater-based MEA solutions containing nickel nanoparticles (NiNPs) as catalysts, with the goal to minimize the amount of MEA required in the amine scrubbing process and eliminate the use of freshwater. This study is the first to use natural seawater solutions as an alternative to freshwater solutions for CO_2 capture. In a microfluidic environment, CO_2 microbubbles were generated and their change in size with respect to time was observed to determine the CO_2 absorption capacity and rate of the test solutions. Pure seawater demonstrated comparable CO_2 absorption to deionized (DI) water. Seawater-based amine solutions absorbed merely 1.79 % less CO_2 than DI water-based amine solutions. Seawater-based amine solutions demonstrated faster CO_2 absorption rates than their freshwater counterparts. Lastly, to further optimize CO_2 absorption, NiNPs were added to each test solution. Seawater with MEA and NiNPs absorbed only 1.15 % less than its DI water counterpart, confirming seawater's potential as amine-based solvent for industrial CO_2 capture applications.

1. Introduction

Excessive anthropogenic CO_2 emissions have driven global temperature rise, ocean acidification, and sea level rise over the last decades [1]. At present, significant quantities of CO_2 emissions are produced by fossil fuel combustion processes in power plants, accounting for 40 % of global CO_2 emissions [2]. Projected CO_2 emissions are expected to substantially exceed sustainable levels, resulting in dangerous long-term consequences for the environment and society [3]. A global temperature increase is associated with more intense precipitation events, including hurricanes, and mass extinction events in a variety of plant and animal species [4]. In addition, due to the continued rise of sea levels and resultant frequent flooding, over 300 million people are estimated to be displaced in the next decades; the economic and political strain caused by this extensive human displacement would be enormous [5]. As global energy demands continue to increase each year, innovative environmentally sustainable methods of power generation that actively address CO_2 emission reduction are essential to combat climate change and mitigate its detrimental effects [6].

Currently, post-combustion CO_2 capture is one of the most prominent technologies being utilized in commercial fossil fuel power plants to reduce their CO_2 emissions [7]. Post-combustion CO_2 capture is the process of removing CO_2 from the flue gas after the combustion process is complete. Typically, the captured CO_2 is then sequestered and stored utilizing complex chemical processes [8]. The modular nature of post-combustion CO_2 capture is a great advantage over other CO_2 capture methods such as pre-combustion carbon capture and oxy-fuel combustion. These methods are comparatively complex and costly to be retrofitted to current power plants [9,10]. Amine scrubbing is the dominant method for post-combustion carbon capture and has already been practically retrofitted to existing power plants [11]. In amine scrubbing, CO_2 rich flue gas and amine solution flow into an absorber unit where the amine solution absorbs CO_2 from the flue gas. After the reaction is complete, the CO_2 depleted flue gas is directed out of the

* Corresponding author.
E-mail address: kimm@fau.edu (M. Kim).

https://doi.org/10.1016/j.jcou.2021.101712
Received 31 May 2021; Received in revised form 4 August 2021; Accepted 6 September 2021
Available online 21 September 2021

absorber unit to be released into the atmosphere. The CO_2 rich amine solution is directed into a regenerator unit where CO_2 is stripped from the amine solution for storage by heating and boiling the solution, and the CO_2 free amine solution is routed back to the absorber unit to be reused [12].

For amine scrubbing in industrial applications, monoethanolamine (MEA) is the predominantly used solvent at concentrations of 15−30 wt % due to its rapid reaction rate, high CO_2 absorption capacity, and excellent thermodynamic stability [13,14]. Despite MEA's effectiveness for CO_2 capture, it presents several drawbacks. First, the use of MEA solvents requires a large amount of freshwater. In some power generation facilities, the freshwater consumption of the facility increases by up to 38 % with the addition of a carbon capture unit [15]. Freshwater demand continues to increase each year, and water scarcity remains to be a problem globally [16]. Almost two-thirds of the world population face severe water scarcity each year [16,17]. As of 2019, 1.1 billion people have no access to clean water, and 2.6 billion have no access to sanitation [17]. Utilizing seawater in amine scrubbing processes can significantly decrease the freshwater consumption of industrial power plants and make amine scrubbing a more sustainable way to address anthropogenic CO_2 emissions. Second, MEA-based solvents produce toxic wastewater that is harmful to the environment and release corrosive fumes that are damaging to power plant equipment [18,19]. Treatment of wastewater containing MEA requires complex chemical processes that are energy intensive and costly [19]. Reducing the necessary concentration of MEA required for amine scrubbing through the use of catalysts would decrease the production of toxic wastewater, and as a result, reduce the total economic and environmental cost associated with amine scrubbing. Lastly, regeneration of MEA during amine stripping (removal of absorbed CO_2 from the solvent) requires significant energy due to the extremely high operation temperature required for CO_2 desorption to occur [19]. 70 % of the total operating costs in a CO_2 capture plant comes from heating required for solvent regeneration. Decreasing the energy required for regeneration of MEA is a primary area of research as it is one of the most effective ways to improve the environmental and economic sustainability of amine scrubbing [19].

In our previous research, we investigated the catalytic activity of nickel nanoparticles (NiNPs) for CO_2 absorption in DI water and aqueous amine solutions [20]. NiNPs were chosen as potential catalysts because of their chemical interaction with aqueous CO_2 that accelerates bicarbonate formation, and because of their high reactivity as a result of their large surface area to volume ratio [20]. In addition, NiNPs have strong resistance to oxidation, corrosion, and thermal degradation, which are essential properties for enduring the standard operating conditions of the amine scrubbing process. We found that NiNPs were effective catalysts, improving CO_2 absorption by 34 % in a limited mixing condition microreactor in DI water [20]. Although NiNPs-based CO_2 capture has shown great potential to replace amine scrubbing, the total CO_2 absorption of this approach still must be improved in order to justify implementing it in industrial applications. Currently, a combined approach utilizing amine solvents and NiNPs as catalysts yields maximum CO_2 absorption [20]. However, the use of substantial amounts of freshwater in this approach must also be reconsidered.

In this paper, we analyze the utilization of seawater-based MEA solvents for CO_2 capture as a possible alternative to currently used freshwater-based MEA solvents. Seawater's ready availability (97 % of Earth's water is seawater) and naturally high CO_2 absorption capacity makes it a promising substitute to freshwater for the amine scrubbing process. To evaluate its CO_2 capture feasibility, we analyze the CO_2 absorption capacity and CO_2 absorption rate of pure seawater and seawater-based amine solvents compared to DI water-based approaches in a microfluidic environment. Additionally, the mechanisms of CO_2 absorption in these solutions are discussed. The potential of NiNPs as a catalyst for CO_2 absorption is also investigated in seawater-based solvents, and the mechanism of NiNPs' catalytic behavior in aqueous solutions is presented. Lastly, the effect of a seawater-based solution on amine solvent regeneration is examined.

2. Materials and methods

A microfluidic approach was utilized to observe and analyze CO_2 absorption in all test solutions. It should be clarified that this paper is not suggesting utilizing microfluidics for industrial amine scrubbing. This is merely the experimental platform that was used to examine the CO_2 absorption capacity of different amine scrubbing solutions. The microbubble-based quantification of CO_2 absorption in microfluidic platforms has been well validated in the literature and provides an excellent experimental framework where variables (e.g., pressure, flow rate) can be easily and precisely controlled [21,22]. A microfluidic approach is also economically and environmentally friendly as it requires significantly less materials and in turn lower cost when compared with conventional experimental methods.

2.1. Materials

Monoethanolamine ($\geq$ 99 % purity) and sodium dodecyl sulfate (SDS, $>$ 99 % purity) were purchased from Alfa Aesar (Ward Hill, MA) and Sigma Aldrich (St. Louis, MO), respectively. Polydimethylsiloxane (PDMS) elastomer kits (Sylgard 184, Dow Corning) were used for fabricating microfluidic chips. NiNPs (Sigma Aldrich, St. Louis, MO) with an average diameter of 100 nm were used in test solutions. Seawater was obtained from the Atlantic Ocean in Boca Raton, Florida with a measured salinity of 35 %. It should be specified that this seawater was from the coast. PDMS microchips were prepared utilizing conventional photolithography methods. (See Supplementary Information (SI) for more details regarding microchannel fabrication).

2.2. Experimental procedure

Gaseous CO_2 was injected into a microfluidic chip with a flow-focusing geometry and serpentine configuration while an aqueous test solution was simultaneously injected (Fig. 1a, b). In the chip, microbubbles were generated at the Y-junction where the aqueous solution flows at an angle of 60 ° relative to the CO_2 gas inlet (Fig. 1c). The synergetic combination of different forces, including inertia, shear, interfacial tension, and pressure forces, creates CO_2 bubbles at microscale in the aqueous solution (Fig. 1d) [23]. The bubble generation frequency can be adjusted by altering the flow rate of the aqueous solution, the relative angle of the aqueous solution to the CO_2 gas inlet, and/or CO_2 gas pressure. The mechanisms of bubble generation in liquid flow have been explored in depth in several microfluidic studies [24,25]. The reduction in the size of CO_2 microbubbles over time was used as an indicator of CO_2 absorption by the surrounding test solution. As more gaseous CO_2 molecules were absorbed by the solution, the size of the microbubbles decreased as CO_2 reacted with MEA and H_2O molecules [20]. A serpentine microchannel configuration was chosen in part because it causes a high degree of mixing, resulting in the increased transfer of CO_2 gas to the aqueous phase [20]. It should be noted that the upper section of the serpentine channel was not visible due to the size of the field-of-view in the imaging system (Fig. 1b). The CO_2 inlet is 50 μm wide while the solvent inlet and the serpentine channel are 100 μm wide. The depth of the channel is 70 μm. Test solutions were pumped into the microfluidic chip using a syringe pump (PHD ULTRA 4400, Harvard Apparatus, Natick, MA) and polytetrafluoroethylene tubing (1/32″I.D.) at a flow rate of 27 μL/min. This flowrate was determined by experimentation and chosen so that a large number of microbubbles were generated at a reproducible steady state. CO_2 gas was injected into the microchannel at 5.5 psig using a pressure regulator (Alicat Scientific, Tucson, AZ) attached to a CO_2 tank (99.9 % purity, Airgas, USA). This pressure was also determined by experimentation and chosen because it supported stable microbubble generation.

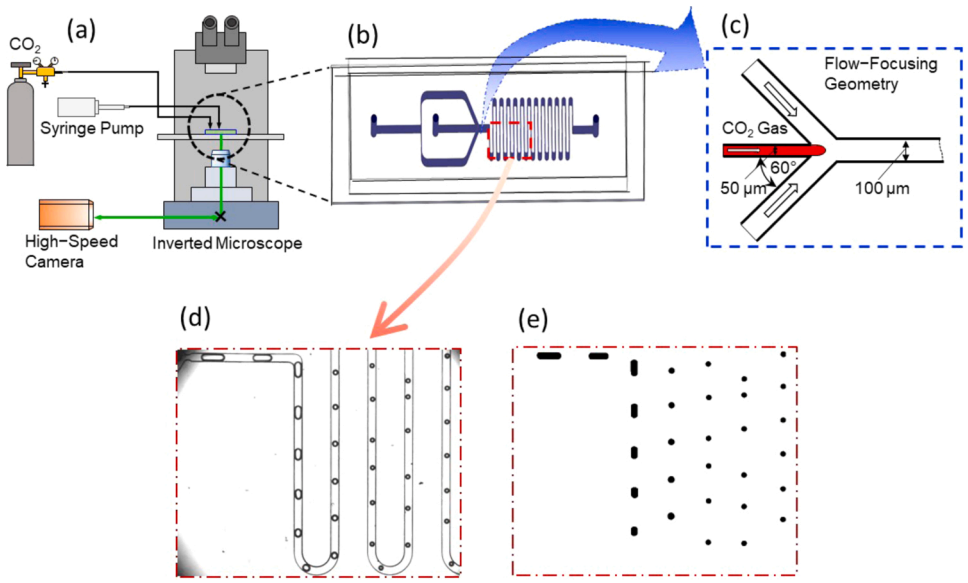

Fig. 1. Schematic of experimental setup and a microfluidic chip. (a) Diagram of experimental setup. (b) Illustrative model of the microfluidic chip. (c) Flow-focusing junction in the geometry where CO_2 bubbles were generated. (d) A raw image showing CO_2 microbubbles in the serpentine microchannel. (e) A processed image to calculate bubble areas.

The CO_2 absorption of DI water and seawater solutions was tested with concentrations of 0%, 1.25 % and 2.5 % MEA (V/V). 0 % MEA DI water served as a control to compare the CO_2 absorption performance of all test solutions. Notably, a precipitate was observed to form as a result of the addition of MEA to seawater. This occurred by the increase in pH of the solution because of the addition of MEA, not as a result of MEA's direct interaction with the precipitated compound. Because MEA was not consumed during the formation of this precipitate, the CO_2 absorption capacity of seawater-based amine solutions were essentially unaffected. This precipitate was filtered from the solution utilizing gravity filtration, and the filtered seawater-based MEA solution was used for experimentation. After the precipitate was filtered, the sample was placed in an oven for one hour at 110 °C to remove any residual moisture content and analyzed using X-ray diffraction. The precipitated compound was identified to be magnesium hydroxide ($Mg(OH)_2$) (See SI).

A maximum concentration of 2.5 % MEA was used for two reasons: 1) In previous research, Seo et al. demonstrated that 5 % MEA in DI water absorbed close to 100 % of CO_2 in a serpentine microfluidic environment [20]. As a result, using concentrations of this magnitude would potentially prevent observation of the total difference in CO_2 absorption capacity between test solutions. 2) MEA is extremely corrosive, and concentrations in excess of 2.5 % MEA rapidly damage (within 15−30 min of continuous experimentation) the PDMS microfluidic chip to the point where the CO_2 microbubbles are unable to be analyzed. It should be noted that this paper is not suggesting the use of 1.25 % or 2.5 % MEA in industrial applications where 15−30 % MEA is the standard. These were simply the concentrations that the experimental framework could support while demonstrating the effect of the amine solvent in the test solutions.

DI water and seawater solutions with concentrations of 0%, 1.25 %, and 2.5 % MEA were also tested with 35 mg/L of NiNPs to observe their catalytic effect. Seo et al. demonstrated previously that this concentration is optimal to maximize the catalytic activity of NiNPs for CO_2 absorption [20]. In all test solutions, the surfactant sodium dodecyl sulfate (SDS) was also used to promote stable CO_2 microbubble generation. The effectiveness of SDS as a surfactant has been demonstrated in previous research at a concentration of 0.25 % and was utilized similarly in this study [20]. SDS reduces the surface tension of the aqueous solution and enlarges the microbubble surface area to volume ratio which allows CO_2 microbubbles to form more easily and reduces the chemical reaction time [20,30]. This increased microbubble formation allows for steady-state experimental conditions that can be easily replicated. Magnetic stirring was used at 750 rpm for 15 min to achieve complete SDS dissolution. All experiments were performed at room temperature at 295.15 K.

2.3. Quantification of CO_2 absorption

The CO_2 absorption in the surrounding solution is proportional to the reduction of CO_2 bubble size over time [26]. Utilizing image processing techniques, the cross-sectional area of each microbubble was calculated, and as a result, the CO_2 absorption as a function of time was found. Once microbubble generation achieved a steady- state, videos of CO_2 microbubbles in the serpentine microchannel were captured with a high-speed camera (Fastec IL5S, Fastec Imaging Corp., San Diego, CA). From the videos, images were selected and analyzed to determine the area and centroid of all CO_2 microbubbles. The ImageJ software was used to identify the bubbles from each original image (Fig. 1e). Then, the number of pixels within each bubble were counted to calculate its respective area. Similarly, the pixel coordinates of each individual bubble's centroid were obtained. Using the coordinates of the centroid of each microbubble relative to a reference point, the distance travelled by each bubble was determined. Then, the time elapsed at each microbubbles' position in the microchannel was calculated using the microbubble's velocity. From this analysis, data sets for time-dependent size-change of CO_2 microbubbles were used to indicate the rate of CO_2 absorption and CO_2 absorption capacity of each test solution. Similar analyses have been adopted in other microfluidic research [27,28].

In our analyses, maximum or final CO_2 absorption was a parameter of interest, making the equilibrium point of the CO_2 absorption reaction critical as well. The reaction was considered at equilibrium when the reduction of the bubble area reached its maximum level and further change in microbubble area was negligible (less than +/- 1 %). The relative CO_2 absorption (% CO_2 absorbed) of each solution is presented rather than the absolute CO_2 absorption (mol/L). This is because it is difficult to maintain the same initial bubble size across all experiments. Using absolute CO_2 absorption in this case would lead to erroneous conclusions. The area of each bubble was determined rather than the volume due to the two-dimensional view of the experimental setup in

addition to the non-spherical nature of initial bubbles in the channel (Fig. 1d). Approximating the volume of these non-spherical initial bubbles would result in additional experimental error. If bubble volume was calculated rather than area, it would not significantly affect experimental results as the final CO_2 absorption would remain essentially the same since the final bubbles can easily be approximated as spherical and thus their volume could be calculated with a high degree of accuracy. In short, if a volume-based approach was utilized results would be approximately identical other than the first few non-spherical bubbles, where small differences could arise. This would only slightly affect the curve fitting performed for reaction rate analysis and have virtually no effect on CO_2 absorption results.

2.4. Statistical analysis

When comparing CO_2 absorption behaviors in two different solutions, student's *t*-test was employed to determine the statistical significance of these differences. A common level of significance (α-value) of 0.05 was selected for all t-testing in addition to 4 degrees-of-freedom. This procedure is elaborated upon in the SI. Additionally, each experiment corresponding to an individual test solution was performed at least three times, and the maximum standard deviation throughout all data sets was calculated to be 1.18 %. For absorption rate analysis, t-testing was not utilized because the decay constant of each solution was not found directly from the experimental data but through the exponential curve fitting of the data. These curve fits had varying R^2 values and, as such, introduce a source of error that would invalidate the *t*-test results. This consistency analysis is also explained in more detail in the SI.

3. Results and discussion

3.1. CO_2 absorption in amine solutions

Fig. 2 presents the CO_2 absorption as a function of time in DI water and seawater solutions with 0 %, 1.25 %, and 2.5 % MEA.

CO_2 absorption in an aqueous solution (without MEA) is largely driven by the formation and dissociation of carbonic acid:

$$CO_{2(g)} \longrightarrow CO_{2(aq)} \tag{1}$$

$$CO_{2(aq)} + H_2O \longrightarrow H_2CO_3 \tag{2}$$

$$H_2CO_3 \longrightarrow H^+ + HCO_3^- \tag{3}$$

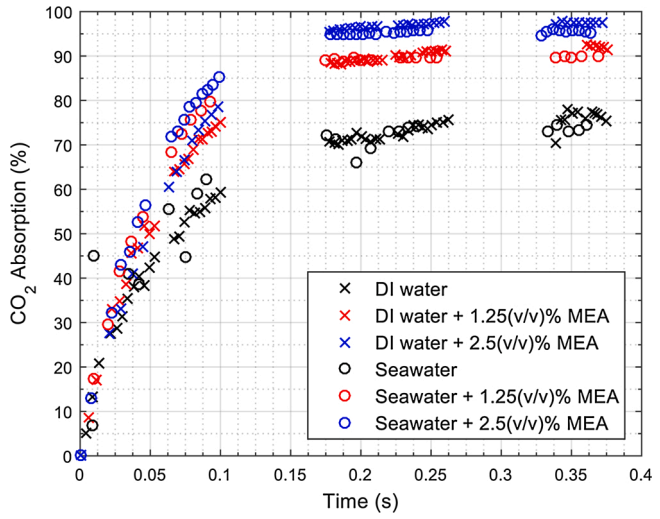

Fig. 2. CO_2 absorption in DI water-based and seawater-based MEA solutions.

$$HCO_3^- \longrightarrow H^+ + CO_3^{2-} \tag{4}$$

This reaction causes an in increase in hydrogen ion concentration until maximum CO_2 absorption (equilibrium) is achieved. The maximum CO_2 absorption in aqueous solutions can be seen in Fig. 2. Pure DI water (0 % MEA) absorbed 78.01 % of CO_2 compared to 74.62 % CO_2 absorption in pure seawater solutions. This result was expected as salinity is negatively correlated with CO_2 absorption [31]. These experimental results are further validated by analyzing the Henry's constant of both solutions. Henry's law states that the solubility of a gas in a liquid (C) is proportional to the partial pressure of the gas (P_g), with the constant of proportionality being denoted as Henry's constant (K_H):

$$C = K_H P_g \tag{5}$$

The partial pressure in all experiments was kept constant at 5.5 psig, and as a result, the calculation of the Henry's constant for each fluid is used as a theoretical basis from which we predict solution CO_2 solubility. The Henry's constant for DI water is well documented by the National Institute of Standards and Technology (NIST) to be 0.034002 M/atm at 295.15 K. The Henry's constant for seawater is calculated from the following temperature and salinity dependent equation given by Emerson and Hedges[32]:

$$K_{H,\,Seawater} = \frac{9345.17}{T} - 60.2409 + 23.3585 ln\left(\frac{T}{100}\right) + S\left[0.023517 - 0.00023656T + 0.0047036\left(\frac{T}{100}\right)^2\right] \tag{6}$$

From Eq. (6), the Henry's constant for seawater is calculated to be 0.03061 M/atm at a temperature of 295.15 K and a salinity (S) of 35 g/L. There is a difference of 9 % between the theoretical Henry's constants of DI water and seawater. Therefore, it is predicted that CO_2 will be slightly more soluble in DI water than in seawater. In experiments, there was an observed difference in maximum CO_2 absorption between pure DI water and seawater of only 3.39 % (approximately 6 % less than theoretically predicted). From this result, it was concluded that seawater demonstrates sufficient intrinsic CO_2 absorption efficiency to be a potentially viable alternative to DI water in the amine scrubbing process. This hypothesis was further evaluated by examining the performance of MEA in DI water and seawater solutions.

With the addition of 1.25 % MEA to DI water and seawater, CO_2 abosprtion was increased by 14.53% and 15.21%, resulting in total CO2 absorption of 92.54% and 89.83%, respectively (Fig. 2). MEA is an extremely effective absorber of CO_2, but it suffers from diminishing returns. The increment in efficiency of MEA is reduced with increased concentration, as seen in our experimental data and similar results found by George and Riverol [33]. Further increasing MEA concentration to 2.5 % in DI water and seawater increased CO_2 absorption by an additional 5.18 % and 6.11 % that the final absorption is to be 97.73 % and 95.94%, respectively (Fig. 2). Seawater solutions demonstrated approximately 1 % greater increases in CO_2 absorption efficiency from the addition of MEA than their freshwater counterparts. This difference in MEA efficiency is relatively insignificant, and as a result, it can be said that the effect of MEA in these test solutions appears to be essentially unaffected by the complex chemical composition of seawater. This leads us to conclude that the dominant reaction mechanism of MEA in seawater (after filtration of the precipitate) is likely to be approximately identical if not totally identical to the reaction mechanism of MEA in DI water. It should be noted that the difference in performance between DI water with 0 % MEA, 1.25 % MEA, and 2.5 % MEA and their respective seawater counterparts was not most likely not due to error and in fact statistically significant ($\alpha = 0.05$).

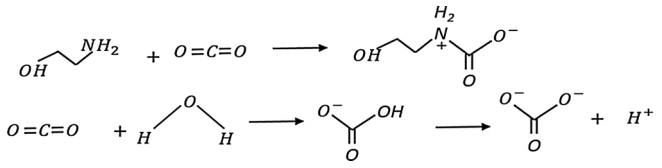

(7a)

(7b)

Eqs. 7a and 7b show the mechanisms of CO_2 absorption in aqueous amine solutions. Eq. (7a) shows CO_2 absorption by MEA due to the production of carbamate while Eq. 7b shows CO_2 absorption by water as a result of the formation and dissociation of bicarbonate ions into carbonate ions, which is dependent on the pH of the solution [34]. A more in-depth aqueous MEA reaction mechanism has been described by Hwang et al. According to their quantum chemical and molecular dynamics study, the reaction mechanism of MEA and CO_2 in aqueous solutions can be explained by three intermediate stages [35].

Stage 1: MEA molecules react with CO_2 and create a zwitterion, a molecule with a positively charged and negatively charged functional group:

$$\mathrm{MEA} + \mathrm{CO_{2(g)}} \longrightarrow MEA^{+}COO^{-} \tag{8}$$

Stage 2: The zwitterion will further deprotonate when it reacts with a H_2O molecule and creates carbamate as well as a solvated proton:

$$MEA^{+}COO^{-} + H_2O \longrightarrow MEACOO^{-} + H_3O^{+} \tag{9}$$

Stage 3: Lastly, the solvated proton reacts with another MEA molecule and creates protonated MEA, thereby capturing CO_2 in the form of stable carbamate:

$$MEA + H_3O^{+} + MEACOO^{-} \longrightarrow MEAH^{+} + H_2O + MEACOO^{-} \tag{10a}$$

Alternatively, there is also the possibility that instead of the reaction shown in Eq. 10a, carbamate will form carbamic acid by reacting with a solvated proton:

$$MEACOO^{-} + H_3O^{+} \longrightarrow MEACOOH + H_2O \tag{10b}$$

3.2. Effect of nickel nanoparticles on CO_2 absorption

To further increase CO_2 absorption of test solutions, NiNP catalysts were utilized. In previous research, NiNPs were shown to be an effective catalyst for CO_2 absorption in aqueous solutions and amine solutions [20]. NiNPs have been proven to effectively enhance CO_2 absorption in DI water independent of pH and to be effective at standard temperature and pressure [20]. NiNPs were predicted to have a similar catalytic effect in seawater solutions, albeit with a mitigated effect due to the salinity and higher pH of seawater. At basic pH, pH dominates CO_2 absorption characteristics of a solution containing significant salinity and the effect of NiNPs are diminished due to the high ionic content of the solution that leads to the NiNPs' aggregation. In contrast, NiNPs show a significant catalytic effect in acidic conditions, regardless of salinity [29]. The pH of seawater used in these experiments was measured to be 7.93, and as a result, NiNPs were predicted to have a mitigated effect in seawater solutions due to the basic environment and salinity of 35 g/L. The catalytic effect of NiNPs for CO_2 absorption is directly a result of their interaction with H_2O:

$$NiNP + H_2O \longrightarrow (NiNP - OH^{-}) + H^{+} \tag{11}$$

$$(NiNP - OH^{-}) + CO_{2(aq)} \longrightarrow (NiNP - HCO_3^{-}) \tag{12}$$

$$(NiNP - HCO_3^{-}) + H_2O \longrightarrow (NiNP - H_2O) + HCO_3^{-} \tag{13}$$

Each nanoparticle reacts with a water molecule to form a hydroxyl group (OH^{-}) on its surface (Eq. 11). A carbonate ion will then form on the surface of a CO_2 microbubble and ultimately shrink its size by subsequent chemical reactions (Eqs. 12 and 13) [20]. Once the solution becomes saturated with bicarbonate ions, NiNPs no longer produce a catalytic effect [36].

Fig. 3 presents the CO_2 absorption performance of all NiNP-assisted test solutions. With the addition of NiNPs, DI water absorbed 8.97 % more CO_2 than pure DI water, achieving 86.98 % maximum CO_2 absorption. In contrast, seawater with NiNPs absorbed 78.30 % of CO_2, an increase of 3.68 % relative to pure seawater. In DI water-based amine solutions, NiNPs increased maximum CO_2 absorption to 94.49 % and 98.20 % with 1.25 % MEA and 2.5 % MEA, respectively. Similarly, seawater-based amine solutions demonstrated very high CO_2 absorption with 92.60 % and 97.05 % CO_2 absorption with 1.25 % MEA and 2.5 % MEA, respectively. The most effective solution for CO_2 absorption was DI water with 2.5 % MEA and NiNPs. However, seawater with 2.5 % MEA and NiNPs was the second most effective CO_2 absorber. It absorbed 97.05 % of CO_2, only 1.15 % less total CO_2 absorption than DI water with 2.5 % MEA and NiNPs. Seawater-based amine solutions enhanced with NiNPs also demonstrated nearly identical CO_2 absorption to the current industry standard, DI water-based amine solutions without NiNPs (97.05 % versus 97.73 %). This difference in performance was determined to be statistically similar ($\alpha = 0.05$). These results further demonstrate the potential viability of NiNP-assisted seawater-based amine solutions for industrial amine scrubbing.

3.3. Influence of amine and nickel nanoparticles on CO_2 absorption rates

In addition to total CO_2 absorbed, the rate of CO_2 absorption by each solution is also a characteristic that was investigated. To perform this analysis, an exponential decay function in the form $A(t) = A_0 e^{-rt}$ was fitted to all experimental data (Fig. 4). From this curve fit, the decay constant of each function was calculated and utilized to compare the reaction rates of solutions.

The R^2 values of the curve fits are shown in Table 1. It should be noted that the curve fit for pure seawater had a significantly lower R^2 value than other test solutions with an R^2 equal to 0.7546 due to high variation in its data. Pure DI water had a slightly suboptimal fit as well

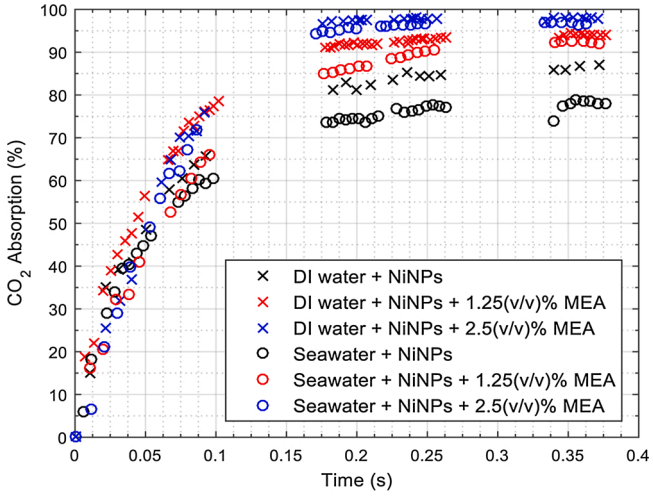

Fig. 3. Effect of NiNPs on CO_2 absorption of DI water and seawater-based MEA solutions.

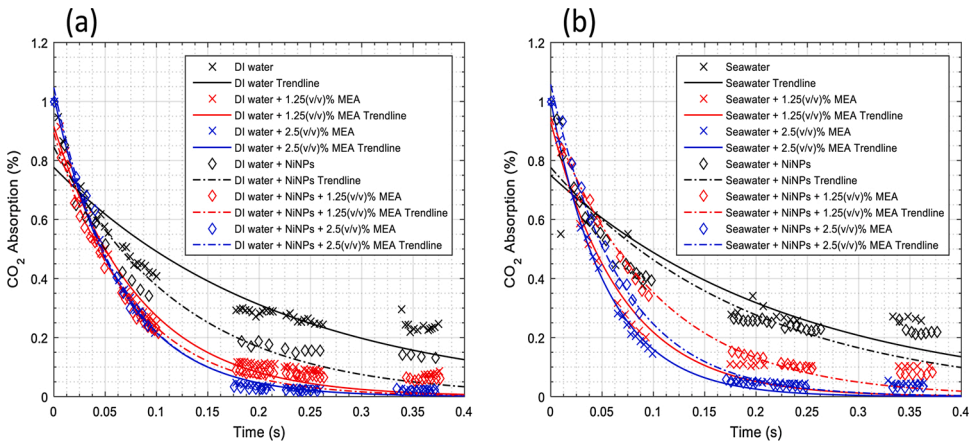

Fig. 4. Exponential decay functions fitted to experimental data. (a) DI water-based solutions' fitted trendlines. (b) Seawater-based solutions' fitted trendlines.

Table 1
Fitted exponential decay functions with corresponding decay rates and R^2 values for all test solutions.

Solutions	Function	Decay Rate	R^2
DI water	$f(x) = 0.7765e^{(-4.566x)}$	4.566	0.8760
DI water + 1.25 %MEA	$f(x) = 0.9156e^{(-12.09x)}$	12.09	0.9685
DI water + 2.5 %MEA	$f(x) = 1.017e^{(-15.47x)}$	15.47	0.9964
DI Water with NiNPs	$f(x) = 0.8455e^{(-8.091x)}$	8.091	0.9322
DI Water 1.25 % MEA with NiNPs	$f(x) = 0.8949e^{(-13.39x)}$	13.39	0.9760
DI Water 2.5 % MEA with NiNPs	$f(x) = 1.047e^{(-15.56x)}$	15.56	0.9918
Seawater	$f(x) = 0.7495e^{(-4.287x)}$	4.287	0.7546
Seawater + 1.25 %MEA	$f(x) = 0.9309e^{(-14.52x)}$	14.52	0.9352
Seawater + 2.5 %MEA	$f(x) = 1.003e^{(-18.36x)}$	18.36	0.9864
Seawater with NiNPs	$f(x) = 0.7762e^{(-5.161x)}$	5.161	0.8641
Seawater 1.25 % MEA with NiNPs	$f(x) = 0.9462e^{(-9.878x)}$	9.878	0.9888
Seawater 2.5 % MEA with NiNPs	$f(x) = 1.058e^{(-14.6x)}$	14.6	0.9945

with an R^2 value of 0.8760. All other solutions had R^2 values greater than 0.9.

As shown in Fig. 4 and Table 1, pure DI water demonstrated a greater absorption rate than seawater with a decay constant of 4.566 versus 4.287. However, in amine solutions, seawater solutions outperformed their DI water counterparts. DI water with 1.25 % MEA and 2.5 % MEA expressed decay constants of 12.09 and 15.47, respectively, compared to seawater solutions with 1.25 % and 2.5 % MEA with decay constants of 14.52 and 18.36, respectively. We believe that the CO_2 absorption rate is greater in these seawater-based amine solutions because of the $Mg(OH)_2$ precipitation. The MEA is not consumed in this process, only protonated (See SI). This may explain why seawater-based amine solutions demonstrated greater CO_2 absorption rates than DI water counterparts. Essentially, the MEA is 'primed' to react with CO_2 by existing in a protonated state.

With the addition of NiNPs, the decay constant of DI water with 0 % MEA, 1.25 % MEA, and 2.5 % MEA increased by 3.525, 1.3, and 0.09, respectively. Pure DI water exhibited the greatest increase in reaction rate due to NiNPs while amine solutions show less significant changes. The decay constant of seawater increased to 5.161 due to the NiNPs' catalytic effect. However, both seawater-based amine solutions with NiNPs demonstrated a reduction in decay constants of -4.642 and -3.76 with 1.25 % MEA and 2.5 % MEA, respectively. We believe these reductions in absorption rates can be attributed to the basic environment of seawater, particularly after the addition of MEA (measured pH of 10.2). As mentioned previously, NiNPs have a diminished effect in high salinity solutions with basic environments [32].

After CO_2 absorption is complete in seawater-based solutions, CO_2 can be removed from the solution and stored through the formation of mineral precipitates such as magnesium carbonate and calcium carbonate. These precipitated carbonate salts can be separated from the solution, and the seawater-based amine solution can then be recycled and reused for further CO_2 capture [37]. If nickel nanoparticles are used as well, they can be easily recollected and reused using magnetic attraction forces without degrading their catalytic ability.

4. Conclusions

Seawater demonstrated its potential for application in industrial amine scrubbing for CO_2 capture with several unique characteristics. First, seawater was observed to demonstrate similar intrinsic CO_2 absorption capacity to DI water. With the addition of the amine solvent, MEA, seawater solutions were observed to absorb up to 95.94 % of CO_2, a difference of less than 2 % with its DI water counterpart. Additionally, the reaction rates of amine solutions were greater in seawater-based solutions than DI water-based solutions. NiNP catalysts were successful in further increasing the performance of seawater-based amine solutions to a maximum of 97.05 % CO_2 absorption. This seawater-based amine solution with NiNP catalysts demonstrated CO_2 absorption performance within less than 1 % of the industry standard DI water-based amine solution (97.05 % versus 97.73 %), a difference that was determined to be statistically insignificant for $\alpha = 0.05$ via student's t-testing. Purely in terms of CO_2 absorption, these results show the viability of seawater-based amine scrubbing, with the added benefit of saving large amounts of freshwater. Additionally, the recycling of NiNPs is not intensive and the seawater-based amine solution with NiNP can be reused for CO_2 absorption. Overall, the proposed seawater-based amine solvent shows unrealized potential that warrants further investigations in large-scale experimental studies.

Author statement

Abhishek Ratanpara: Conceptualization, Methodology, Experiments, Writing, Editing; **Alex Shaw:** Methodology, Experiments, Writing, Reviewing, Editing; **Mallory Thomas:** Methodology, Experiments, Writing, Reviewing, Editing; **Rajesh Patel:** Consultation, Editing; **Myeongsub Kim:** Conceptualization, Methodology, Writing, Reviewing, Editing

Declaration of Competing Interest

The authors declare that they have no known competing financial interests or personal relationships that could have appeared to influence the work reported in this paper.

Acknowledgements

We extend our gratitude to Dr. Masashi Kurashina and Dr. Alberto Haces for their guidance and chemistry expertise. We gratefully acknowledge Sanat Deshpande for his help in laboratory experiments and his remarks on literature review. We also would like to thank Gabriel Scharf for contributing his analytical chemistry knowledge towards the identification of the observed precipitate. This work has been partially supported by Florida Environmental Studies Janke Research Funds.

References

[1] N.R. Bates, M.H.P. Best, K. Neely, R. Garley, A.G. Dickson, R.J. Johnson, Detecting anthropogenic carbon dioxide uptake and ocean acidification in the North Atlantic Ocean, Bio Geosci. Discuss. 9 (1) (2012) 989–1019, https://doi.org/10.5194/bgd-9-989-2012.

[2] H. Yang, Z. Xu, M. Fan, R. Gupta, R.B. Slimane, A.E. Bland, I. Wright, Progress in carbon dioxide separation and capture: a review, J. Environ. Sci. 20 (1) (2008) 14–27, https://doi.org/10.1016/S1001-0742(08)60002-9.

[3] M. Grubb, F. Sha, T. Spencer, N. Hughes, Z. Zhang, P. Agnolucci, A review of Chinese CO_2 emission projections to 2030: the role of economic structure and policy, Clim. Policy 15 (January 2016) (2015) 7–39, https://doi.org/10.1080/14693062.2015.1101307.

[4] R.A. Pielke, C. Landsea, M. Mayfield, J. Laver, R. Pasch, Hurricanes and global warming, Bull. Am. Meteorol. Soc. 86 (11) (2005) 1571–1575, https://doi.org/10.1175/BAMS-86-11-1571.

[5] D. Ebbing, S. Gammon, General chemistry (ed. 11).

[6] M.K. Mondal, H.K. Balsora, P. Varshney, Progress and trends in CO_2 capture/separation technologies: a review, Energy 46 (1) (2012) 431–441, https://doi.org/10.1016/j.energy.2012.08.006.

[7] B. Lv, B. Guo, Z. Zhou, G. Jing, Mechanisms of CO_2 capture into monoethanolamine solution with different CO_2 loading during the absorption/desorption processes, Environ. Sci. Technol. 49 (17) (2015) 10728–10735, https://doi.org/10.1021/acs.est.5b02356.

[8] Y. Wang, L. Zhao, A. Otto, M. Robinius, D. Stolten, A review of post-combustion CO_2 capture technologies from coal-fired power plants, Energy Procedia 114 (November 2016) (2017) 650–665, https://doi.org/10.1016/j.egypro.2017.03.1209.

[9] P. Bouillon, S. Hennes, C. Mahieux, CO_2: post-combustion or Oxyfuel – a comparison between coal power plants with integrated CO_2 capture, Energy Procedia 1 (1) (2009) 4015–4022, https://doi.org/10.1016/j.egypro.2009.02.207.

[10] Laurence Tock, François Maréchal, Process engineering method for systematically comparing CO_2 capture options, Comput. Aided Chem. Eng. 32 (2013), https://doi.org/10.1016/B978-0-444-63234-0.50062-2. Elsevier.

[11] J.D. Figueroa, T. Fout, S. Plasynski, H. McIlvried, R.D. Srivastava, Advances in CO_2 capture technology-the U.S. department of energy's carbon sequestration program, Int. J. Greenh. Gas Control. 2 (1) (2008) 9–20, https://doi.org/10.1016/S1750-5836(07)00094-1.

[12] M. Stec, A. Tatarczuk, L. Wie, Pilot plant results for advanced CO_2 capture process using amine scrubbing at the Jaworzno II Power Plant in Poland, Fuel (January) (2015) 1–7, https://doi.org/10.1016/j.fuel.2015.01.014.

[13] J.I. Huertas, M.D. Gomez, N. Giraldo, J. Garzón, CO2 absorbing capacity of MEA, J. Chem. 2015 (2) (2015), https://doi.org/10.1155/2015/965015.

[14] K.A. Mumford, Y. Wu, K.H. Smith, G.W. Stevens, Review of solvent based carbon-dioxide capture technologies, Front. Chem. Sci. Eng. 9 (2) (2015) 125–141, https://doi.org/10.1007/s11705-015-1514-6.

[15] G. Magneschi, T. Zhang, R. Munson, The impact of CO_2 capture on water requirements of power plants, Energy Procedia 114 (November 2016) (2017) 6337–6347, https://doi.org/10.1016/j.egypro.2017.03.1770.

[16] Food and Agriculture Organization of the United Nations (FAO), 2021. http://www.fao.org/3/a-i6459e.pdf.

[17] The United Nation Word Water Report, 2019. https://reliefweb.int/sites/reliefweb.int/files/resources/367306eng.pdf.

[18] P. Luis, Use of monoethanolamine (MEA) for CO_2 capture in a global scenario: consequences and alternatives, Desalination 380 (2016) 93–99, https://doi.org/10.1016/j.desal.2015.08.004.

[19] J. Jung, Y. Su, Y. Lim, C. Seob, Advanced CO_2 capture process using MEA scrubbing: configuration of a split flow and phase separation heat exchanger, Energy Procedia 37 (2013) 1778–1784, https://doi.org/10.1016/j.egypro.2013.06.054.

[20] S. Seo, B. Lages, M. Kim, Catalytic CO_2 absorption in an amine solvent using nickel nanoparticles for post-combustion carbon capture, Journal of CO2 Utilization 36 (August 2019) (2020) 244–252, https://doi.org/10.1016/j.jcou.2019.11.011.

[21] S. Seo, M. Mastiani, M. Hafez, G. Kunkel, C. Ghattas Asfour, K.I. Garcia-Ocampo, et al., Injection of in-situ generated CO_2 microbubbles into deep saline aquifers for enhanced carbon sequestration, Int. J. Greenh. Gas Control. 83 (October 2018) (2019) 256–264, https://doi.org/10.1016/j.ijggc.2019.02.017.

[22] J. Park, Z. Nie, A. Kumachev, E. Kumacheva, A microfluidic route to small CO_2 microbubbles with narrow size distribution, Soft Matter 6 (2010) 630–634, https://doi.org/10.1039/b914572a.

[23] L. Sheng, Y. Chen, K. Wang, J. Deng, G. Luo, General rules of bubble formation in viscous liquids in a modified step T-junction microdevice, Chem. Eng. Sci. 239 (2021), 116621, https://doi.org/10.1016/j.ces.2021.116621.

[24] T. Cubaud, M. Sauzade, R. Sun, CO_2 dissolution in water using long serpentine microchannels, Biomicrofluidics 6 (2012), 022002, https://doi.org/10.1063/1.3693591.

[25] S. Arias, D. Legendre, R. Gonzales-Cinca, Numerical simulation of bubble generation in a T-junction, Comput. Fluids 56 (2012) 49–60, https://doi.org/10.1016/j.compfluid.2011.11.013.

[26] S. Seo, G. Perez, K. Tewari, X. Comas, M. Kim, Catalytic activity of nickel nanoparticles stabilized by adsorbing polymers for enhanced carbon sequestration, Sci. Rep. 8 (2018) 11786, https://doi.org/10.1038/s41598-018-29605-1.

[27] M. Hafez, A. Ratanpara, Y. Martiniere, M. Dagois, Ghazvini, M. Kavosi, P. Mandin, M. Kim, CO_2-monoethanolamine-induced oil swelling and viscosity reduction for enhanced oil recovery, J. Pet. Sci. Eng. (2021), https://doi.org/10.1016/j.petrol.2021.109022.

[28] S. Shim, J. Wan, S. Hilgenfeldt, P. Panchal, H. Stone, Dissolution without disappearing: multicomponent gas exchange for CO_2 bubbles in a microfluidic channel, Lab Chip 14 (2014) 2428, https://doi.org/10.1039/c4lc00354c.

[29] S. Seo, M. Nguyen, M. Mastiani, G. Navarrete, M. Kim, Microbubbles loaded with nickel nanoparticles: a perspective for carbon sequestration, Anal. Chem. 89 (20) (2017) 10827–10833, https://doi.org/10.1021/acs.analchem.7b02205.

[30] C. Devos, Effect of sodium dodecyl sulfate on the continuous crystallization in microfluidic devices using microbubbles, Chem. Eng. Technol. (10) (2019) 1–9, https://doi.org/10.1002/ceat.201900172.

[31] M. Al-hindi, F. Azizi, Absorption and desorption of carbon dioxide in several water types, Can. J. Chem. Eng. 96 (July 2017) (2020) 274–284, https://doi.org/10.1002/cjce.22901.

[32] S. Emerson, J. Hedges, Chemical Oceanography and the Marine Carbon Cycle, Cambridge University Press, Cambridge, 2008, https://doi.org/10.1017/CBO9780511793202.

[33] E.C. George, C. Riverol, Effectiveness of Amine Concentration and Circulation Rate in the CO_2 Removal, 2020, pp. 1–17, https://doi.org/10.1002/ceat.201900233.

[34] R.E. Zeebe, D. Wolf-Gladrow, CO_2 in Seawater: Equilibrium, Kinetics, Isotopes, 1st edition, Elsevier, 2001, pp. 1–10. ISBN: 0 444 50579 2.

[35] G.S. Hwang, H.M. Stowe, E. Paek, D. Manogaran, Reaction mechanisms of aqueous monoethanolamine with carbon dioxide: a combined quantum chemical and molecular dynamics study, Phys. Chem. Chem. Phys. 17 (2) (2015) 831–839, https://doi.org/10.1039/c4cp04518a.

[36] G.A. Bhaduri, L. Šiller, Nickel nanoparticles catalyse reversible hydration of carbon dioxide for mineralization carbon capture and storage, Catal. Sci. Technol. 3 (5) (2013) 1234–1239, https://doi.org/10.1039/c3cy20791a.

[37] D. Kang, Y. Yoo, J. Park, Accelerated chemical conversion of metal cations dissolved in seawater-based reject brine solution for desalination and CO_2 utilization, Desalination 473 (2019), https://doi.org/10.1016/j.desal.2019.114147.